INTERNATIONAL JOURNAL OF
COASTAL, OFFSHORE & ENVIRONMENTAL ENGINEERING

Available online at: www. ljcoe.org

Investigation of the pitch motion of a semi-submersible offshore platform combining conventional mooring systems using genetic algorithms

Farshid Azizi[1], Saeid Kazemi[2*], Farhood Azarsina[3]

[1] Ph.D. student, Department of Engineering, Science and Research Branch, Islamic Azad University, Tehran, Iran; farshid.azizi@srbiau.ac.ir
[2] Assistant Professor, Department of Engineering, Science and Research Branch, Islamic Azad University, Tehran, Iran; Saeid.kazemi@srbiau.ac.ir*
[3] Assistant Professor, Department of Engineering, Science and Research Branch, Islamic Azad University, Tehran, Iran; f.azarsina@srbiau.ac.ir

ARTICLE INFO

Article History:
Received….
Accepted ….
Available online ….

Keywords:
Catenary mooring
Taut mooring
Semi-submersible platform
Optimization motion response
Genetic Algorithm

ABSTRACT

The Mooring systems play a significant role in the hydrodynamic behaviour of the floating offshore platforms. This research examines the role of mooring systems in regulating the pitch motion of semi-submersible platforms, given their growing application in deep-water operations. Excessive platform movements can compromise structural stability and operational performance. To analyze platform motion, numerical simulations of the AmirKabir semi-submersible platform were conducted under various mooring configurations using nonlinear time-domain analysis. Two optimization approaches were employed: a numerical trial-and-error method and a genetic algorithm based on stochastic selection, both utilizing numerical modeling to define the fitness function. The predicted outcomes from the genetic algorithm align with those obtained from numerical methods in reducing platform pitch motion. Three mooring configurations derived from the genetic algorithm demonstrate an approximately 32% improvement over numerical models. The results indicate that combining catenary and taut mooring lines yields optimal behavior in controlling the pitch motion of semi-submersible platforms.

1. Introduction

Oceans and seas furnish essential natural resources, such as crude oil and natural gas beneath the seabed. Floating structures designed for exploration and extraction in deep waters have gained popularity with recent discoveries of large offshore oil and gas fields. Over the past decades, the demand for floating platforms (including Floating Production Storage and Offloading units (FPSOs), semi-submersibles, spars, and tension-leg platforms) has increased. A critical component of these floating platforms is the mooring system, crucial for preserving the structure's position under specific environmental conditions to safely conduct operations like drilling, extraction, offloading, and power generation (e.g., offshore wind turbines). Designing such systems presents difficulties for engineers across various aspects, including design, engineering, construction, installation, operation, inspection, monitoring, maintenance, and repair [1].

As illustrated in Figure 1, a semi-submersible platform is a specialized floating structure designed for offshore drilling, oil extraction, heavy lifting, accommodation, or a combination of these functions. Once oil wells are drilled and completed by drilling vessels, semi-submersible platforms are deployed to the field and connected to permanent mooring systems. Semi-submersibles are stable and cost-effective platforms. As offshore oil and gas development has progressed into deeper waters, the use of semi-submersible platforms has become increasingly popular due to their large deck space for accommodating heavy equipment

and the ease of integrating the topside structure alongside the quay.

Figure 1. Semi-submersible platform [2].

Marine moorings are crucial components of floating platform station-keeping systems developed for offshore oil and gas exploration and extraction. Beyond anchoring the floating structure at a designated location, the mooring system restricts platform movements to ensure the integrity and performance of drilling and production facilities, such as production risers, drilling risers, and their centralization. Marine mooring systems can be designed for a wide range of conditions, from harsh environments like the North Sea to milder settings like the Gulf of Thailand or West Africa, and for water depths ranging from a few meters to over 3,000 meters.

Mooring systems can be classified as either catenary or taut, depending on their profiles and configurations. As illustrated in Figure 2, a catenary mooring system features a mooring line profile in which part of the line lies statically on the seabed due to its own weight. These systems are commonly used, particularly in shallow to moderate water depths.

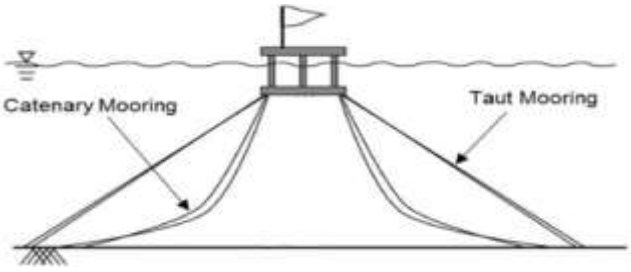

Figure 2. Types of tensile-catenary mooring systems [3].

In contrast, a taut mooring system does not have any portion of the line resting on the seabed; instead, the lines stretch directly from anchors on the seabed to fairleads on the floating structure. As a result, taut mooring systems have a smaller operational radius and require shorter lines compared to catenary systems. However, because the lines are taut, the platform's offset and dynamic responses are more significantly affected by line tension. In shallow water, this can lead to excessive stiffness and an undesirably high line tension. Therefore, taut mooring systems are more suitable for deep or ultra-deep water applications. Typically, a semi-submersible platform uses 8, 12, or 16 mooring lines, arranged evenly in four groups and connected from four columns to the seabed [4].

Extensive research has been conducted on analyzing and optimizing mooring lines for offshore platforms. In one study, Hermawan and Furukawa investigated the dynamic behavior of multi-component mooring lines for analyzing the motion of a floating offshore structure. They developed a coupled three-dimensional dynamics model using the lumped mass method, allowing the motion of segment connection points and including anchors and clump weights. This model facilitates the analysis of simultaneous interlocking-segment line motions to solve three-dimensional dynamic responses of multi-component mooring lines. The model integrates hydrodynamic loads, line-seabed interaction, elasticity, current effects, and dragging anchor motions. It is coupled with a ship-type floating offshore structure and validated by comparing it with equivalent models based on conventional numerical methods. The study concluded that the model could successfully provide realistic predictions of the motion of floating structures and highlighted the significant impact of lateral mooring line motion on mooring line tension [5].

In another study, Feng et al. developed and examined a model for dynamic mooring lines by integrating a boundary element model for a two-dimensional floating body with a coupled mooring line model. The boundary model was formulated in the time domain using the Rankine approach, and a reflection potential was introduced to simulate wave reflection caused by seabed slope. This newly developed model was validated through comparisons with available data. Subsequently, the dynamic response analysis was conducted under different seabed conditions. Compared to a flat seabed, a sloping seabed induced asymmetrical configurations in the mooring lines and caused significant effects on the motion responses of the floating body [6].

In another study, Trubat et al. investigated the mooring forces of floating offshore wind turbines primarily driven by platform motions through yaw motion. Conventional dynamic analyses typically consider only the hydrodynamic mooring forces induced by wave-generated linear motion. Using the FloaWDyn aero-servo-hydro-elastic model, the impact of wave hydrodynamic loads on catenary lines and the platform system was assessed and simulated for various sea states, both with and without wave forces. Stress variations and increases in standard deviation were analyzed across multiple scenarios. It was found that the extended tension range of the mooring system (by 5% under extreme sea conditions) affects damage during mooring load events and compromises the fatigue resistance of the mooring lines [7].

In another study, Okoubaka et al. applied a genetic algorithm to assess the feasibility of optimizing the geometry and dimensions of a floating platform designed to host sloped wave energy converters. In this research, frequency-domain analysis was used to conduct sensitivity tests regarding the search starting point, selection of optimized variables, number of iterations, simulation time, and the contents of the search space. The results indicated that the number of iterations required for convergence increases with the number of optimized variables. Furthermore, for the studied platform geometry, no universally optimal unit was identified. Instead, various combinations of characteristic features in response to wave forces were comparatively evaluated. Ultimately, it was observed that when the solution space is controlled and contains a subset of known potential solutions for improving system performance, computation time, energy absorption efficiency, and the range of improvement are enhanced. Additionally, the optimized genetic algorithm tends to favor platform geometries for which the wave resonance response aligns with dominant wave climate frequencies. A key contribution of this study lies in the controlled manipulation of the variable space for a subset of potential solutions that enhance system performance. This controlled approach leads to improvements in computational time, energy absorption efficiency, and the optimal operational state of the platform [8].

In another investigation, Mariares Casimiro et al. proposed a novel framework for the multi-objective optimization of mooring systems for floating renewable energy platforms by employing a surrogate model based on random forest algorithms combined with a genetic algorithm. This framework, applied to the optimization of the mooring system for a floating wind turbine, demonstrates how this approach can support strategic design decision-making in real-world problems faced by the renewable energy sector. The framework utilizes validated numerical models of the mooring system to train the surrogate model, resulting in an efficient computational optimization routine that enables exhaustive exploration of the search space. This framework presents a wide range of optimal solutions and illustrates how design changes affect the trade-offs between two competing objectives, while also minimizing both cost and cumulative fatigue of the mooring system [9].

Youliang Zhao et al. investigated the design and optimization of a mooring system for a floating platform—a task that typically relies heavily on engineering experience and time-consuming numerical simulations. A novel hybrid approach, BPNN-FEM, combining a Back Propagation Neural Network (BPNN) and a modified Finite Element Method (FEM) model, was proposed to facilitate more efficient statistical prediction and dynamic stress series forecasting in mooring systems with multiple design variables under irregular sea states. The accuracy of this approach was validated using several statistical error metrics. This method offers a more cost-effective alternative to intensive numerical simulations for optimizing the design of floating platform systems. An optional mooring configuration was proposed based on maximum safe operations, drift constraints of the platform, and the safety performance of mooring lines. A semi-submersible platform deployed in deep water was used as a case study to demonstrate the proposed hybrid approach. The platform consisted of twelve mooring lines, and the design variables included the mooring radius, azimuthal spacing of the mooring lines, and lengths of various segments of the mooring lines. Environmental loads were also considered in this optimization process. The predicted results aligned well with those obtained through the FEM [10].

Currently, numerous studies are being conducted on the mooring of offshore platforms. Each researcher considers specific environmental and structural conditions to enhance platform mobility and improve mooring performance. Based on the unique capabilities of each mooring type, this study investigates the combined use of taut and catenary moorings,

independently, to improve the pitch motion of an offshore semi-submersible platform. The objective is to identify an optimal combination that minimizes platform motion as effectively as possible.

In this article, we analyzed the pitch motion of a semi-submersible offshore platform and employed the Genetic Algorithm (GA) as an optimization tool for the analysis and design process. Pitch motion is considered one of the critical parameters in the performance of semi-submersible platforms and is influenced by factors such as wind forces, wave action, and ocean currents. Based on the conducted analysis, it was found that accurately modeling this type of motion requires complex modeling and precise computation. Therefore, the use of artificial intelligence techniques such as the Genetic Algorithm demonstrates high potential in optimization and identifying influential parameters. By simulating the natural processes of selection and inheritance, the Genetic Algorithm is capable of conducting a more targeted search within the solution space and providing acceptable results.

In this study, various methodologies for simulating and analyzing pitch motion were investigated, and several strategies were proposed to enhance the accuracy and efficiency of the analyses. The results demonstrated that employing the Genetic Algorithm significantly reduces prediction errors and improves the operational conditions of offshore platforms.

Ultimately, the findings of this research not only contribute to a deeper understanding of pitch motion in semi-submersible platforms but also serve as a reference for future studies and the development of optimization techniques in the oil and gas industry. In general, future research may focus on the integration of artificial intelligence algorithms with hydrodynamic modeling to achieve improved outcomes in this field.

2- Governing Equations

A semi-submersible platform, as an offshore structure, is governed by hydrodynamic and structural equations. These equations are used to analyze the displacement behavior and platform responses to environmental forces and motions [11]. A floating structure in open waters is subjected to environmental loads resulting from wind, waves, currents, ice, and other factors [12-13]. Figure 3 illustrates the effects of wind, current, and waves. These forces are among the most significant environmental parameters that influence the motion of the floating structure. The mooring system is designed to provide control over the structure in response to these external and internal forces.

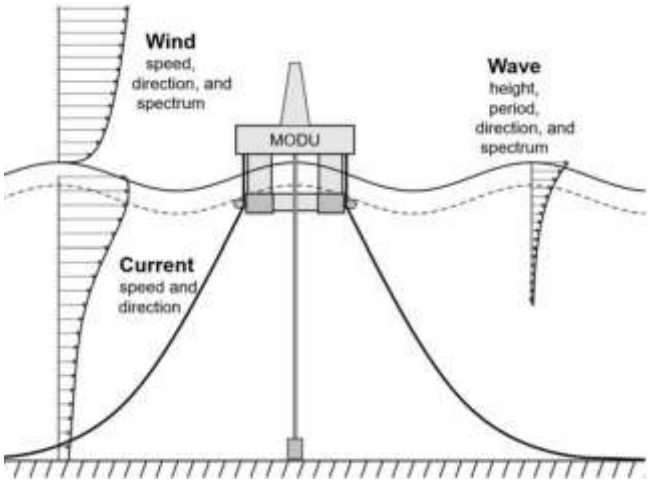

Figure 3. Wind, wave and current forces on a floating platform [1]

2-1- Motion Equation for a Semi-Submersible Platform

The motion equation for a floating vessel consists of three rotations (roll, pitch, and yaw) and three translations (surge, sway, and heave) along the x, y, and z axes. For analyzing and modeling motion for a semi-submersible vessel under different forces, the motion equation is given as:

$$M(p.a) + C(p.v) + K(p) = F(p.v.t) \qquad (1)$$

Where:

M is the inertia matrix of the structure

C is the damping matrix

K is the restoring force matrix

F is the external force vector acting on the structure

p, v, a, and t are the vectors for position, velocity, acceleration, and time, respectively

2-2- Wind Load

The wind force acting on a semi-submersible platform can be calculated using the following equation [1]:

$$F = \frac{1}{2}\rho V_p^2 C_D A \qquad (2)$$

Where:

ρ is the air density

V_p is the wind speed

C_D is the drag coefficient of the platform's surface

A is the projected area of the platform exposed to wind

2-3- Hydrodynamic Forces

The hydrodynamic forces exerted on floating structures can be divided into categories according to wave frequency:

— Sustained wave-frequency forces, which are always present and have a magnitude and direction that does not change over an amount of time and lead to wave drift forces. Such fixed loads cause the floating object to be pushed in one direction and are counteracted by the restoring force from moorings [1].

— Oscillating wave-frequency forces, whose periods average from 5 up to 30 seconds. Such forces cause periodic stresses within the structure, which give rise to maximum mooring line tensions and fatigue damage accumulation within the mooring system. Anchors and risers in some conditions exert extra damping in the floating body's movements, including surge, sway, and roll motions [13].

— Low-frequency wave loads affect floating platform components such as the mooring system, typically within the time range of 180 to 600 seconds [14].

The maximum wave load on marine structures occurs at the wave frequency, causing the floating structure to oscillate at that frequency. To avoid large resonance effects, marine structures and their mooring systems are generally designed such that their resonance frequencies lie well outside the structure's natural frequency range. Wave-induced loads can trigger high-frequency elastic responses, and due to nonlinear load effects, some responses may still occur at natural frequencies [15].

Hydrodynamic loads were calculated using the classical Morison equation, in which ρ is the water density, C_D the drag coefficient, C_M the inertia coefficient, R^{γ} the dimension of the element (diameter for a cylindrical section, width or length for a rectangular section), u the water particle velocity, a the particle acceleration, x the displacement of the member, and z the vertical coordinate of the node.

$$F_{hydro}(z) = \rho C_d R|u - \dot{x}|(u - \dot{x}) + \pi\rho R^2 a + (C_M - 1)\pi\rho R^2(a - \ddot{x}) \quad (3)$$

2-4- Damping

Damping effects were considered using classical Rayleigh damping as defined in Equation (4). Rayleigh damping is a linear combination of mass and stiffness. Here, the damping matrix C is defined as:

$$C = \mu M + \lambda K \quad (4)$$

In Equation (4), M and K are the mass and stiffness matrices, respectively, and μ and λ are proportionality constants. Figure 4 shows how the damping ratio varies with frequency. This graph demonstrates the contribution of mass and stiffness damping to the total damping ratio.

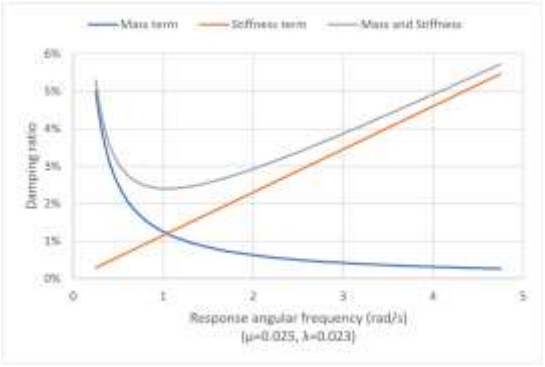

Figure 4. Change in damping ratio [16]

Rayleigh damping coefficients must be carefully selected to avoid the excessive damping of low-frequency responses caused by the mass-proportional damping component. It is also important to note that mass damping can induce damping due to the rigid-body motions of the floating structure. Therefore, mass-proportional damping is generally neglected. In other words, for such systems, the use of stiffness-proportional damping (upper red curve) is recommended [16].

Natural frequencies and critical damping are essential parameters for analyzing floating body motions. Resonance occurs when the period of an external

excitation force approaches the natural period of the floating system. The natural frequency f and the critical damping BC of a floating system, as functions of total mass (M + Ma) and stiffness K in six degrees of freedom, are defined as follows:

$$Natural\ frequency: f = \sqrt{\frac{K}{M + M_a}} \quad (5)$$

$$Critical\ damping: B_C = 2\sqrt{(M + M_a)K} \quad (6)$$

2-5- Mooring Lines Governing Equations

Figure 5 illustrates a small element of the mooring line in a two-dimensional plane (x-z coordinate system). In the free-body diagram shown, P represents the submerged weight per unit length, T the effective tension, dl the length element, AE the axial stiffness, dψ the normal displacement, and dφ the tangential displacement of the mooring line.

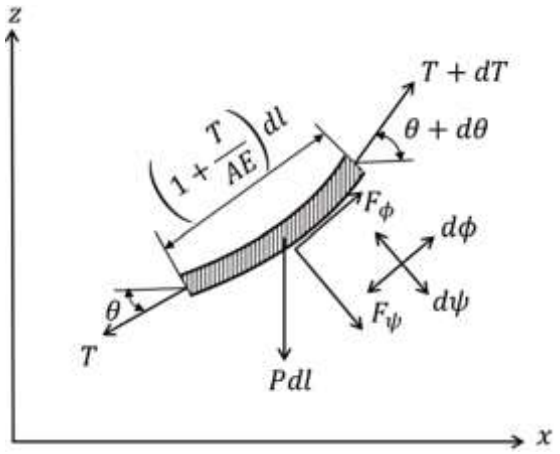

Figure 5. Force and displacement on an element of the mooring line [1]

In mooring line design, it is assumed that the bending and torsional stiffness of the line are negligible—an assumption considered valid for chains and for wire or polyester ropes with a large curvature radius and broadly accepted in the industry [17]. The effects of the hydrodynamic forces Fφ and Fψ on the mooring are calculated using Morison's equation. The governing differential equations for computing the forces on the mooring lines take into account both dynamic and elastic effects. These equations are nonlinear and require numerical simulations for accurate solutions [18-19].

2-5-1- Static Mooring Equations

The static equations of mooring lines were first formulated by Leibniz, Huygens, and Bernoulli in 1691[20-21]. The solution to the catenary equation has a hyperbolic cosine function form. In dynamic load calculations on mooring lines, damping and inertial forces are neglected due to their small magnitude. It is assumed that the mean horizontal environmental force (due to wind, wave, and current) applied at the mooring connection point is T_0. The reference frame origin (x_0, z_0) is placed at the seabed contact point of the mooring line, where the line's slope is zero, as shown in Figure 6. Here, l_s is the suspended length (arc length) of the mooring line, l_t the total mooring length, and h the vertical distance from the starting point to the seabed.

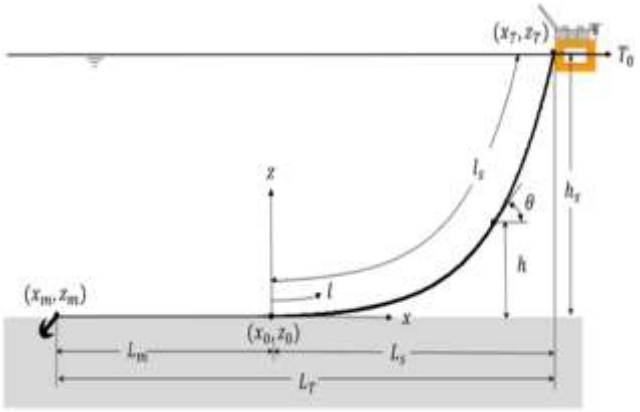

Figure 6. Geometric characteristics of the catenary line [1]

For simplicity in calculation, mooring elements are assumed inelastic; i.e., for a homogeneous catenary mooring line, AE = ∞, which gives:

$$dT - P\ sin\theta\ dl = 0 \quad (7)$$

$$T\ d\theta - p\ cos\theta\ dl = 0 \quad (8)$$

These equations are derived from the above relations when seabed boundary conditions are applied:

$$l(x) = \frac{T_0}{P} sinh\left(\frac{P}{T_0}x\right) \quad (9)$$

$$h(x) = \frac{T_0}{P} cosh\left(\frac{P}{T_0}x\right) - \frac{T_0}{p} \quad (10)$$

From Equations (9) and (10), for a given horizontal tension T_0, we can plot the mooring line configuration.

Within the suspended range, for which $0 < l < l_s$, we have:

$$l = \sqrt{h\left(h + 2\frac{T_0}{P}\right)} \qquad (11)$$

To calculate tension along this section, we use the following relation:

$$T(l) = T_0 + P\,h \qquad (12)$$

For a chain-type catenary mooring line, Equation 12 shows that static chain tension along the fairlead increases linearly with environmental force and is equal to the horizontal force plus the weight of the chain when submerged. For moorings that are taut and do not have load-bearing capacity in the direction of elevation, an estimate of the minimum required length for moorings to prevent uplift is essential, which can be derived from the following relation between total length *l* and total tension T.

$$l = h\sqrt{\left(2\frac{T}{P\,h} - 1\right)} \qquad (13)$$

Based on Equations (9) and (10), the preferred approach for force resistance is with inelastic catenary lines. Next, including elastic stretch in them, one can find quasi-static solutions for multi-material catenary lines [22-23].

2-5-2- Mooring line stiffness

A mooring line exerts horizontal and vertical forces, denoted by T_H and T_v respectively, on the floating structure, as defined in Equations (14) and (15).

$$T_H = (T_H)_M + k_{11}\eta_1 \qquad (14)$$
$$T_v = (T_v)_M + k_{33}\eta_3 \qquad (15)$$

In Equations (14) and (15), η_1 and η_3 represent motions, while k_{11} and k_{33} denote the stiffness in the horizontal and vertical directions, respectively. Both T_H and T_v are related to the offset of the floating structure. The greater the displacement of the structure from its equilibrium position, the greater the reaction force T_H will be. Similar to a simple spring system, this relationship between the structure's offset and the mooring line's reaction force is referred to as mooring stiffness. Mooring stiffness represents a proportional relationship between force and displacement. When the line tension increases significantly, the mooring line experiences both axial elongation and overall geometric deformation. Therefore, mooring stiffness consists of both axial stiffness (AE) and geometric stiffness components [24].

2-5-3- Mooring Line Dynamics

Equation (16) describes the tension in a mooring line resulting from wave-frequency (WF) motion:

$$M\frac{d^2r}{dt^2} + B\frac{dr}{dt} + K\,r = F(r.t) \qquad (16)$$

In Equation (16), M is the added mass, B is damping, K is the stiffness matrix, F is an external excitation force, and *r= (x.y.z)* is the displacement vector from the equilibrium position. The dynamic analysis, which includes added mass, damping, and stiffness, is illustrated in Figure 7.

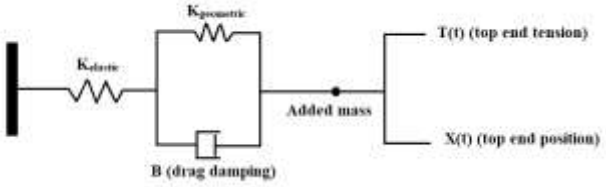

Figure 7. Illustration of a dynamic analysis for a catenary mooring line

2-5-4- Mooring Systems General Design

As shown in Figure 8, a mooring system is connected to a semi-submersible structure using multiple lines.

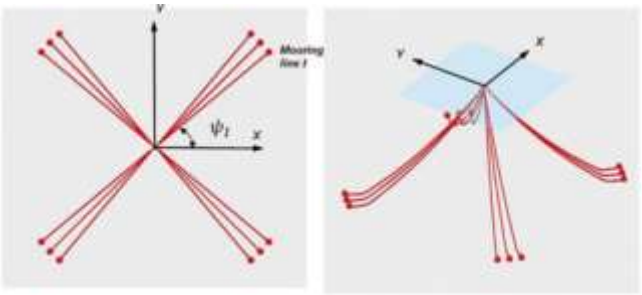

Figure 8. Multiple-line mooring system [1]

The motion of the floating structure can be described using the equations of motion in six degrees of freedom:

$$\sum_{j=1}^{6}\left[\left(M_{ij}+M_{aij}\right)\frac{d^2\eta_j}{dt^2}+B_{Lij}\frac{d\eta_j}{dt}+B_{Q_{ij}}\left|\frac{d\eta_j}{dt}\right|\frac{d\eta_j}{dt}+K_{ij}\eta_j\right]=F_i \quad (17)$$

In Equation (17), the indices *i* and *j* denote the direction of hydrodynamic force and the mode of motion, respectively. *i* = 1-2-3-4-5-6 correspond to surge, sway, heave, roll, pitch, and yaw. B_L and B_Q represent linear and quadratic damping coefficients, respectively. The right-hand side of Equation (17) includes environmental forces (mean wind, wave, and current forces) [23-25].

On the left-hand side of Equation (17), Ma represents added mass (in-phase with acceleration), along with the damping and stiffness contributions of the mooring lines. For the stiffness matrix K and damping matrix B, the total contribution from mooring lines is the sum of all individual lines. For instance, the surge-direction contribution can be calculated using the following relation:

$$Surge: K_{11}=\sum_{I=1}^{n}k_1cos^2\psi_I \quad (18)$$

$$Sway: K_{22}=\sum_{I=1}^{n}k_1sin^2\psi_I \quad (19)$$

2-6- Genetic Algorithm

The genetic algorithm is a specific type of evolutionary algorithm that utilizes evolutionary biology techniques such as inheritance, biological mutation, and Darwinian principles of selection to find an optimal formula for prediction or pattern matching. Genetic algorithms are often a good option for regression-based prediction techniques. As illustrated in Figure 9, genetic evolution is used as a problem-solving model in genetic algorithm modeling [8]. The problem to be solved has inputs that are transformed into solutions through a process modeled on genetic evolution. These solutions are then evaluated as candidates using a fitness function. If the termination condition is met, the algorithm stops. In general, the genetic algorithm is an iterative algorithm in which many of the components are selected via stochastic processes [26].

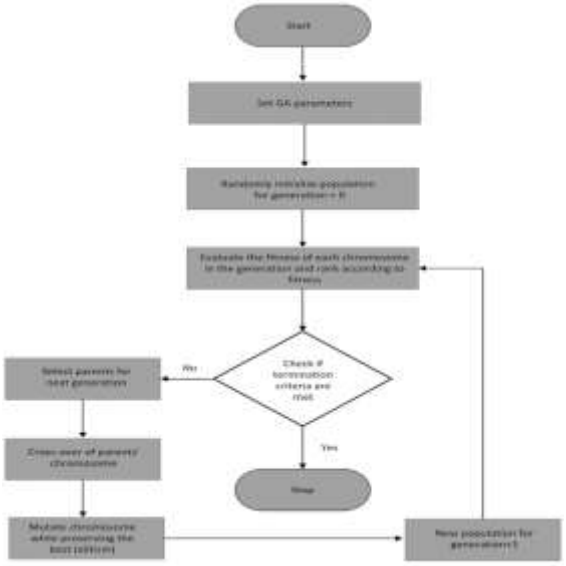

Figure 9. Flowchart of the steps of the genetic algorithm [8]

3- Simulation

Simulation, as a powerful tool in engineering sciences, allows us to model and analyze the behavior and performance of systems and processes under actual or desired conditions. Through simulation, we can enhance the predictive capability and performance optimization of a system without the need for costly and time-consuming experiments. Numerical simulation enables us to perform a wide range of analyses related to mooring lines and floating platforms within a simulated environment. Finite element simulation is used for analyzing moorings and dynamic analysis within the OrcaFlex software [27]. Mooring analysis is performed by dividing the mass of the system into discrete nodes, treated as point masses connected by springs [28-29]. Initially, the geometry of the structure and moorings is modeled in a three-dimensional environment. Then, the model is divided into smaller linear elements (for moorings) and surface elements (for the platform). For each element, material properties, boundary conditions, and other required parameters are defined. Using the governing equations for linear and surface elements, the response of each element at every time step is computed. The results of individual elements are then combined to obtain the overall structural response.

The structure considered in this paper is the Amirkabir semi-submersible platform, which was developed from the GVA-4000 basic design and is positioned 250 km off Neka Port, Iran, in the Caspian Sea. The overall shape and structural parameters of the Amirkabir platform are depicted in Figure 10 and Table 1.

Figure 10. AmirKabir Semi-submersible platform

Table 1. Geometrical specifications of the Amirkabir semi-submersible platform [30-31].

Description	Value	Description	Value
Width (m)	78.84	Length (m)	98.6
Pantone length (m)	80.56	Height to deck floor (m)	28.5
Pantone width (m)	18.68	Height to deck ceiling (m)	36.5
Brace diameter (m)	2	Column diameter (m)	12.9
Draught (m)	19.5	Distance between columns (m)	54.72
Operating weight	28,621	Fairlead height (m)	11.2

The Amirkabir semi-submersible platform is designed with eight mooring lines, each three kilometers in length (two mooring lines at each corner of the platform). This involves the use of long and complex mooring systems, which can result in challenges such as high costs, complexity of installation, maintenance difficulties under varying weather conditions, and technical and physical constraints. The mooring specifications are presented in Figure 11 and Table 2.

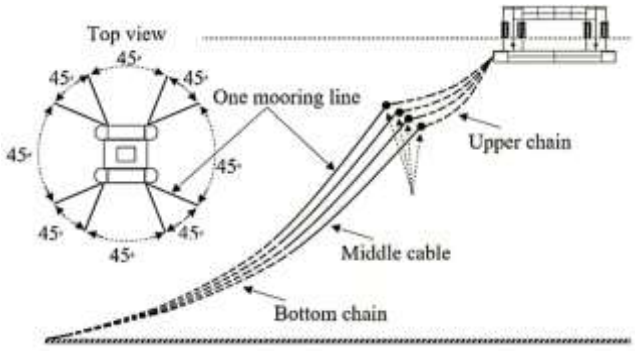

Figure 11. AmirKabir semi-submersible platform mooring specifications [32]

Table 2. Specifications of a mooring for the Amirkabir semi-submersible platform [33]

Fracture strength KN	Quality	Length (m)	Diameter (mm)	Type	Section
MBL5454	NV–R3S	900	76	Chain	Top
MBL5100	IWRS37*6	1000	86	Cable	Middle
MBL5454	NV– R3S	1100	76	chain	Bottom

3-1- Environmental Data Collection

For modeling the semi-submersible platform and calculating the forces, accurate and consistent environmental data must be used (data presented in this section were collected by the consulting company Owj Pajoohesh Sanat'e Iran). The air density is taken as 0.0013 te/m³, and the kinematic viscosity of air used for Reynolds number calculations is considered as 15×10^{-6} m²/s. The seabed is assumed to be smooth and elastic, with a design depth of 500 meters for this platform. The specifications of environmental forces (wave, wind, and current) used in the software are listed in Table 3 [32-34].

Table 3. Environmental forces of the Caspian Sea [32-33]

Type	Value		Angle	Description
JONSWAP	T_z	H_s	180	**Wave**
	12.8 s	9.5 m		
NPD	22 m/s		180	**Wind**
Interpolated	0.86 m/s		180	**Curent**

3-2- Model Validation

Following the geometric modeling and definition of environmental conditions and applied forces, the software's validity is evaluated. In the context of floating structure design, the Response Amplitude

Operator (RAO) is an engineering statistic used to determine the probable behavior of a floating body when subjected to sea forces. RAOs, typically derived from tested models in wave tanks or from specialized computational CFD software (such as ANSYS), represent how a structure responds to incoming wave energy at various frequencies.

As shown in Figure 12, in this context, RAO results obtained from existing ANSYS simulations of the Amirkabir platform in six degrees of motion from three angles are carefully recorded.

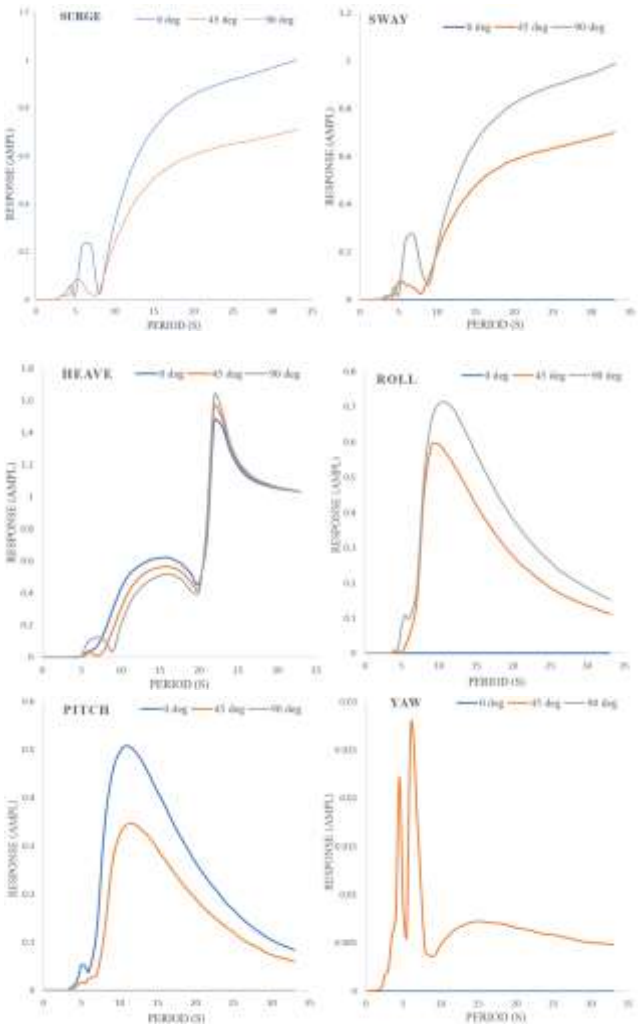

Figure 12. Response spectrum range of the Amirkabir semi-submersible platform

Interpolation techniques were used to compute the remaining angles. Then, the forces are input, and the Amirkabir semi-submersible platform is modeled in OrcaFlex software. To ensure that the RAOs from ANSYS align with those of the simulated platform and input forces, the output spectral RAOs from OrcaFlex are then compared with previously obtained data. The validation steps are as follows:

1. Input of existing RAOs
2. Modeling of platform and moorings
3. Input of environmental forces
4. Examination of output RAOs
5. If matched, validation is confirmed; otherwise, model parameters are adjusted accordingly

In OrcaFlex, the input RAOs, platform specifications, mooring lines, and environmental forces are fixed and unchangeable; however, the output RAOs vary depending on all the aforementioned fixed parameters. In cases of discrepancy, to minimize differences between input and output RAOs, model-level variables such as connectors and similar details (without altering the main form of the platform, moorings, or environmental forces) are adjusted through trial and error. As shown in Figure 12, the RAOs of the simulated platform are presented. Thus, by disregarding minor errors, the results in Figures 12 and 13 are considered acceptable and largely consistent.

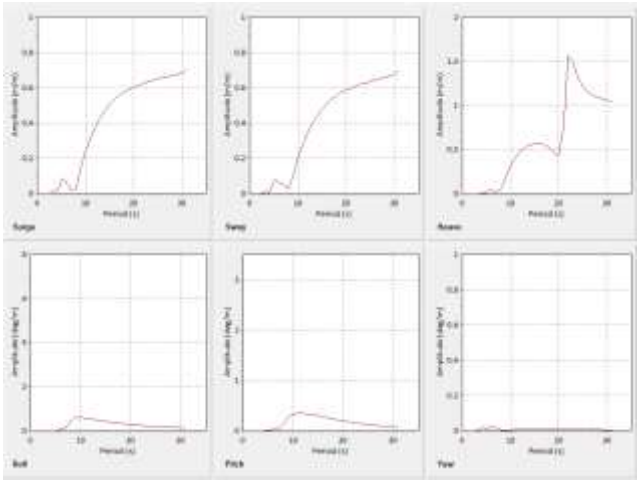

Figure 13. Response spectrum amplitude at 45 degree angle

The similarity between the two graphs can be further increased by maintaining modeling accuracy and continuously improving simulation criteria in OrcaFlex.

3-3- Modeling

3-3-1- Numerical Modeling

Various configurations of the Amirkabir semi-submersible platform with different numbers of

mooring lines (4, 8, 12, and 16) are examined in this section.

As shown in Figure 14, the initial model assumes the platform with eight mooring lines (two per corner) as the baseline. Subsequently, by changing the length and placement of the moorings, alternative models of the Amirkabir platform are created.

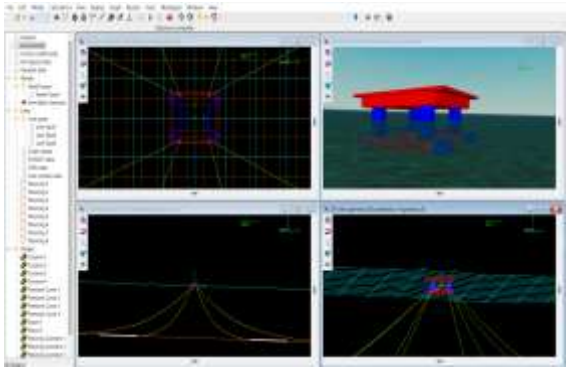

Figure 14. Model of the Amir Kabir semi-submersible platform with Orcaflex software

After running each model, time-displacement graphs are extracted to analyze the platform's pitch motion. Then, using Fast Fourier Transform (FFT), the time-displacement data are converted into dimensionless RAO amplitude spectra graphs. These graphs illustrate the platform's displacement over time, and pitch angles are used to analyze these graphs.

Given that each of the Amirkabir platform's mooring lines consists of three segments (catenary – taut – catenary), in the conducted models, each mooring is modeled using a single material and simplified as a one-piece element (either catenary or taut). The pre-tension forces of the moorings are determined based on relevant standards and the specific requirements of the Amirkabir platform.

The following modifications were applied in the numerical modeling to improve the mooring performance:

- Reducing taut mooring length
- Reducing vertical connection angle
- Reducing catenary length
- Optimizing anchor location
- Altering horizontal angles

Using OrcaFlex, a total of 30 different mooring configurations were tested on the Amirkabir platform. The catenary mooring length was set to 2000 meters and the taut section to 700 meters. The number of moorings varied from one to four per column of the semi-submersible platform.

The 30 initial models included:

1. Two 4-mooring (4×1) configurations
2. Four 8-mooring (4×2) configurations
3. Eight 12-mooring (4×3) configurations
4. Twelve 16-mooring (4×4) configurations

Each model was created in OrcaFlex and the respective time-displacement graphs were extracted. Figure 15 presents the pitch motion response graphs of the 30 configurations.

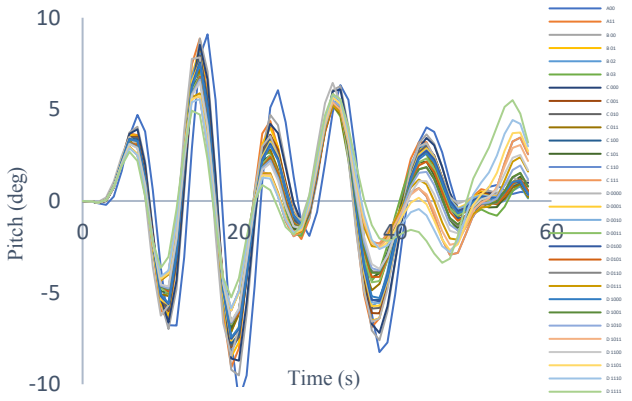

Figure 15. Time-displacement diagrams of 30 numerical models at the pitch movement angle

3-3-2- Modeling Using Genetic Algorithm

Following the numerical modeling and corresponding outputs, the genetic algorithm was employed to further improve the pitch motion of the platform. Initially, the pitch motion outputs of the 30 numerical models described previously were encoded using a neural network based on the mooring specifications of each platform. The specifications of the neural network are presented in Tables 4 and 5.

Table 4. Neural network specifications

Data Division	Random (dividerand)
Training	Levenberg-Marquardt (trainlm)
Performance	Mean Squared Error (mse)
Calculations	MEX

The output of this neural network served as the initial fitness function in the genetic algorithm's coding. In this implementation, the optimization was prioritized based on the degree of rotational motion in the pitch direction. In other words, parent models that exhibited less pitch motion were prioritized and their traits were passed on to the next generation. Given that the operation of the genetic algorithm is based on random selection, two output iterations were generated for a more robust evaluation. Each output iteration proposed a significant number of semi-submersible platforms with different mooring configurations. Figures 16 and 17, along with Table 5, illustrate the neural network regression and genetic algorithm parameters for the two output iterations.

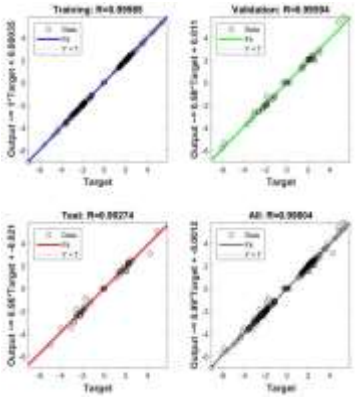

Figure 16. Neural Network Regression Run1

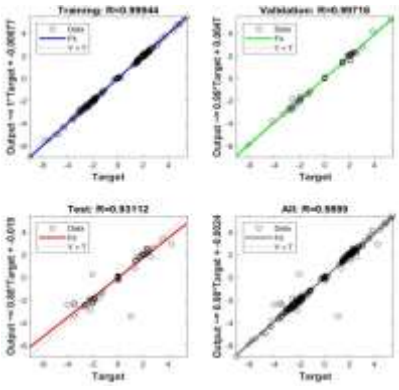

Figure 17. Run2 neural network regression

As regulated by the genetic algorithm, the optimization paths for each of the two iterations are manifested in Figure 18. As can be noticed, in both iterations, the objective function improved from a higher to a lower value and dropped from approximately 7–8 to values near 5–6.

As regulated by the genetic algorithm, the optimization paths for each of the two iterations are manifested in Figure 18. As can be noticed, in both iterations, the objective function improved from a higher to a lower value and dropped from approximately 7–8 to values near 5–6.

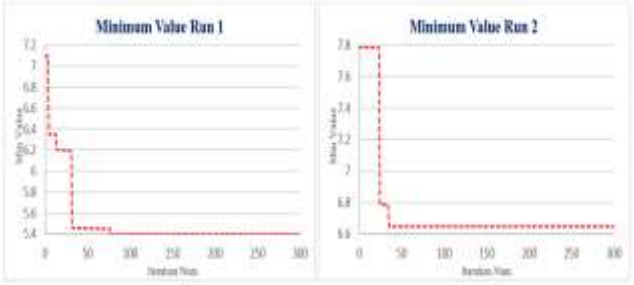

Figure 18. Minimize diagram of two-period genetic algorithm

According to the objective function in Figure 18, each output of the genetic algorithm generated 2,000 mooring configuration models for the semi-submersible platform. From each set, six models with better pitch motion performance were selected based on the number of moorings, resulting in a total of twelve selected models. Each of these models was subsequently simulated under defined conditions, and the pitch motion outputs were analyzed for the configurations proposed by the genetic algorithm.

Table 5. Characteristics of the four-output neural network of the genetic algorithm

	Unit	Epoch	Performance	Gradient	Mu	Validation Checks
Run 1	Initial Value	0	1.4	2.15	0.001	0
	Stopped Value	47	0.000644	0.00491	1.00E-05	6
	Target Value	1000	1.00E-07	1.00E+10	6	6
Run 2	Initial Value	0	1.67	2.63	0.001	0
	Stopped Value	12	0.000869	0.00366	1.00E-05	6
	Target Value	1000	0	1.00E-07	1.00E+10	6

4- Results

4-1- Numerical Modeling Results

In the initial stage of numerical modeling, by applying static and dynamic loads, the platform reached an equilibrium state and displacements were reduced. However, over time, amplification in the platform's motion fluctuations was observed. Based on minimum displacement, four out of the thirty numerically modeled platforms simulated in OrcaFlex were selected, as listed in Table 6. Their response amplitudes were identified and compared to the original Amirkabir semi-submersible platform. The mooring characteristics of these four optimized models are also described in Table 6. For simplicity and better comprehension, all tables describing mooring specifications only include the moorings connected to one column located in the first quadrant of the four-column configuration.

Table 6. Characteristics of the restraints of the selected models in numerical modeling

Model name		Specifications moorings				
		Number of mooring lines	Type	Radius	Length	Azimuth angle
C 110	3	line 1	Taut	521	700	22.5
		line 2	Taut	521	700	45
		line 3	Catenary	1860	2000	67.5
D 0111	4	line 1	Catenary	1848	2000	30
		line 2	Taut	519	700	40
		line 3	Taut	519	700	50
		line 4	Taut	519	700	60
D 1101	4	line 1	Taut	520	700	30
		line 2	Taut	520	700	40
		line 3	Catenary	1848	2000	50
		line 4	Taut	520	700	60
D 1110	4	line 1	Taut	522	700	30
		line 2	Taut	522	700	40
		line 3	Taut	522	700	50
		line 4	Catenary	1847	2000	60

Using Fourier series, the time-displacement graphs of the models were converted into Response Amplitude Operator (RAO) graphs. In offshore platforms, three directions are of particular importance: surge, heave, and pitch. Figure 19 shows the pitch RAO spectra of the four numerical models alongside the pitch RAO spectrum of the Amirkabir semi-submersible platform.

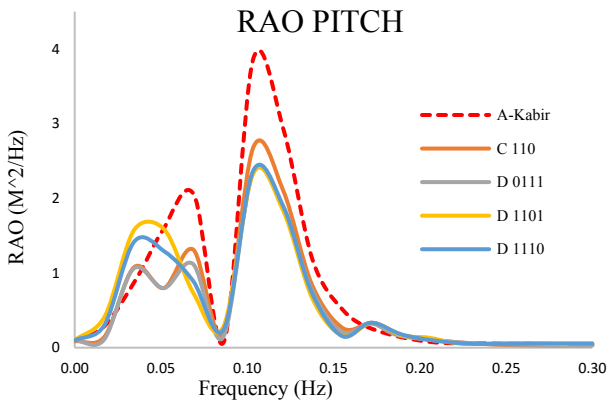

Figure 19. Comparison chart and examination of the response amplitude spectrum of the screw movement of numerical models

A considerable reduction in pitch motion was proven through the graphs, which verified acceptable and favorable optimization. However, for optimizing the models further, one of the best-suited optimization algorithms, (the genetic algorithm), was utilized in the following step.

4-2- Genetic Algorithm Modeling Results

This section analyzes the performance of the twelve models given by the genetic algorithm, previously described. Based on two groups of outputs and comparison between motion graphs derived from simulations made in OrcaFlex, three superior models were identified. The mooring specifications of these chosen models from the genetic algorithm are given in Table 7. The pre-tension and mean tensile forces for all three catenary and taut moorings are further given in Figure 20.

Table 7. Characteristics of the constraints of the genetic algorithm output models

Models	Num Line	Catenary %	Taut %	L Catenary (m)	L Taut (m)	Azimuth			
						C1	T1	T2	T3
D1-1	4	25%	75%	1,742	551	68	68	55	69
C1-2	3	33%	67%	1,683	522	43	21	28	-
D1-2	4	25%	75%	1,757	560	40	41	42	44

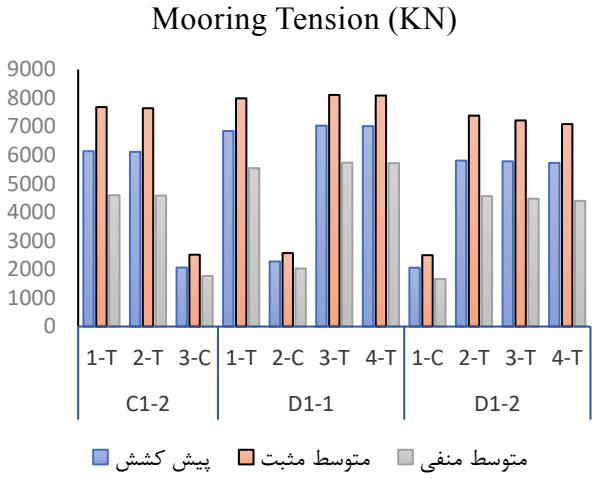

Figure 20. Restraint force of the final optimal motion models

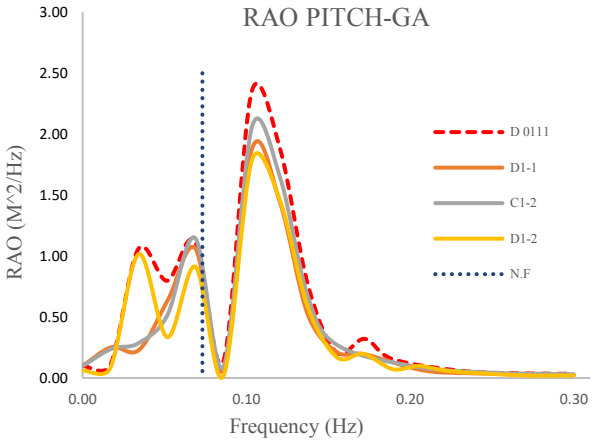

Figure 21. Comparison chart and examination of the response amplitude spectrum of the screw movement of genetic algorithm models

Figure 20 displays the forces on the moorings on one side of the four-sided platform, with the taut moorings labeled as T and the catenary moorings as C. By modeling the configurations proposed by the genetic algorithm in OrcaFlex, their time-displacement graphs were obtained. These were then converted into RAO graphs and compared with the best numerical model. Figure 21 presents comparative RAO pitch motion spectra of the best genetic algorithm-based models. These graphs include the numerical model D0111 (the optimal numerical model) and the genetic algorithm-based models C1-2, D1-1, and D1-2.

As seen in the figure, all genetic algorithm models outperform the optimal numerical model in terms of pitch motion. By comparing and analyzing the RAO spectra of the optimized and initial models, and considering the significance of the peak response location relative to the natural frequency due to the risk of resonance, the critical role of mooring optimization on platform behavior becomes clearer. According to Figure 21, the peak RAO responses lie within a favorable frequency range relative to the natural frequency.

4-3- Two Modeling Methods Comparison

The results of platform motion variations due to different mooring configurations were evaluated under both numerical and genetic algorithm-based modeling. In this section, for each model, mooring variations and their relation to platform displacements over time were analyzed, with a focus on catenary and taut moorings. Based on the modeling described earlier, four numerical and three genetic algorithm-based models were ultimately selected. Their mooring configurations

were compared to the Amirkabir semi-submersible platform in Table 8.

Table 8. Percentage reduction in anchorage length and operating radius of anchorages of numerical models and genetic algorithm compared to the Amirkabir semi-submersible platform

Manual Models	Percentage reduction		GA Models	Percentage reduction	
	Mooring length	Operating radius		Mooring length	Operating radius
C 110	41%	36%	D1-1	43%	44%
D 0111	32%	36%	C1-2	55%	47%
D 1101	32%	36%	D1-2	43%	44%
D 1110	32%	36%			

The results from modeling demonstrate that adjustments in mooring number and position have a considerable impact on the pitch motion characteristics of the semi-submersible platform. An increase in mooring number lessened platform displacement while maximizing its stiffness and stability.

These results, as displayed in Table 9, further illustrate that mooring configurations vary the stability and strength of the platform in all directions. The percentage reduction in pitch motion for genetic algorithm-based models relative to the best numerical model is given in Table 9.

Table 9. Percentage improvement in motion changes of genetic algorithm models compared to the best numerical model (D0111)

Method	Models	Pitch
Genetic Algorithm	D1-1	32%
Genetic Algorithm	C1-2	28%
Genetic Algorithm	D1-2	31%

As seen, D1-1 proved to perform optimally in relation to platform displacement. This model, which was proposed by the genetic algorithm, has 16 moorings (twelve taut and four catenary). The changes made in moorings greatly enhanced motion behavior of the platform compared to the original one. The mooring changes resulted in a remarkable reduction in motion behavior in terms of the platform's pitch motion.

5- Conclusion

From modeling and displacement analyses, we can see clearly that changes in mooring number, length, and position relative to the original design model have a direct bearing upon the behavior and displacement of the platform.

One of the main changes applied in the models was the adjustment, enhancement, and reduction of moorings. The findings indicate that utilizing a single type of mooring (either catenary or taut) yields better platform motion performance than using a combination of both. This design strategy enhances the platform's strength and stability when faced with harsh marine environmental conditions. In summary, mooring modifications significantly improved the platform's performance and stability. Utilizing these optimized models minimizes the risk of unwanted vibrations and oscillations in the platform. These improvements in the semi-submersible platform's motion enhance its strength and stability during operation.

Moreover, analyzing the time-displacement graphs can reveal how displacements evolve over time, which can aid in improving the platform design and enhancing its safety. The modeling of the Amirkabir semi-submersible platform with various mooring configurations using the genetic algorithm clearly demonstrated the direct influence of mooring type and position on platform behavior and displacement. Given the responsiveness of optimization algorithms in the offshore industry, their application can lead to meaningful advancements in the design and optimization of semi-submersible platforms. The mooring optimization conducted here resulted in significant improvements in platform performance and structural integrity.

For future research, other salient parameters influencing semi-submersible platform motion, specifically for moorings, can be explored—e.g., different depths, column geometry, and pontoons. Further accuracy can be achieved through refining modeling and analysis procedures, as well as pursuing an exploration of the remaining five degrees of motion.

6- References

1- Ma, K. T., Luo, Y., Kwan, C. T. T., & Wu, Y. (2019). *Mooring system engineering for offshore structures*. Gulf Professional Publishing. https://doi.org/10.1016/C2018-0-02217-3

2- Karlsson, D., & Forser, M. (2015). Structural analysis of node cut-outs in a semi-submersible offshore platform. https://doi.org/10.1115/OMAE2016-54068

3- Lee, J., Kwon, O., Kim, I., Kim, G., & Lee, J. (2019). Cyclic pullout behavior of helical anchors for offshore floating structures under inclined loading condition. *Applied Ocean Research*, *92*, 101937. https://doi.org/10.1016/j.apor.2019.101937

4- Wang, R. (2016). *Design of mooring systems in extreme seastates with focus on viscous drift force modelling* (Master's thesis, NTNU). http://hdl.handle.net/11250/2622949

5- Hermawan, Y. A., & Furukawa, Y. (2020). Coupled three-dimensional dynamics model of multi-component mooring line for motion analysis of floating offshore structure. *Ocean Engineering*, *200*, 106928. https://doi.org/10.1016/j.oceaneng.2020.106928

6- Feng, A., Kang, H. S., Zhao, B., & Jiang, Z. (2020). Two-Dimensional Numerical Modelling of a Moored Floating Body under Sloping Seabed Conditions. *Journal of Marine Science and Engineering*, *8*(6), 389. https://doi.org/10.3390/jmse8060389

7- Trubat, P., Molins, C., & Gironella, X. (2020). Wave hydrodynamic forces over mooring lines on floating offshore wind turbines. *Ocean Engineering*, *195*, 106730. https://doi.org/10.1016/j.oceaneng.2019.106730

8- Ekweoba, C., El Montoya, D., Galera, L., Costa, S., Thomas, S., Savin, A., & Temiz, I. (2024). Geometry optimization of a floating platform with an integrated system of wave energy converters using a genetic algorithm. *Renewable Energy*, 231, 120869. https://doi.org/10.1016/j.renene.2024.120869

9- Reyes-Casimiro, M., Félix-González, I., & Perea, T. (2023). Design optimization for production semi-submersible pontoons based on genetic algorithms and finite element analysis. *Ocean Engineering*, 268, 113291.
https://doi.org/10.1016/j.oceaneng.2022.113291

10- Zhao, Y., Dong, S., Jiang, F., & Incecik, A. (2021). Mooring tension prediction based on BP neural network for semi-submersible platform. *Ocean Engineering*, *223*, 108714. https://doi.org/10.1016/j.oceaneng.2021.108714

11- Zhang, Z. L., Yuan, H. T., Sun, S. L., & Ren, H. L. (2021). Hydrodynamic characteristics of a fixed semi-submersible platform interacting with incident waves by fully nonlinear method. *International Journal of Naval Architecture and Ocean Engineering*, *13*, 526-544. https://doi.org/10.1016/j.ijnaoe.2021.06.003

12- Mazarakos, T., & Tsaousis, T. (2024). Hydrodynamic Loads on a Semi-Submersible Platform Supporting a Wind Turbine Under a Mooring System With Buoys. *Polish Maritime Research*, *31*(1), 24-34. https://doi.org/10.2478/pomr-2024-0003

13- Larsen, K. (2015). *Fatigue Analysis and Design of Mooring Systems. Assessment and comparison of different methods* (Master's thesis, NTNU). http://hdl.handle.net/11250/2350726

14- Jonkman, J. M. (2007). *Dynamics modeling and loads analysis of an offshore floating wind turbine*. University of Colorado at Boulder.

15- Eslahi, M. J., Ezam, M., & Ghodsi Hassanabad, M. (2023). Numerical Study on Heave Plate Effects on Hydrodynamic Responses of Floating Offshore Wind Turbines. *Journal Of Marine Engineering*, *19*(41), 119-133. http://marine-eng.ir/article-1-1070-en.html

16- Zerwer, A., Cascante, G., & Hutchinson, J. (2002). Parameter estimation in finite element simulations of Rayleigh waves. *Journal of geotechnical and geoenvironmental engineering,* 128(3), 250-261. https://doi.org/10.1061/(ASCE)1090-0241(2002)128:3(250)

17- Sarpkaya, T. (1966). Experimental determination of the critical Reynolds number for pulsating Poiseuille flow.

18- Schulz, K. W., & Kallinderis, Y. (2000). Three-dimensional numerical prediction of the hydrodynamic loads and motions of offshore structures. *J. Offshore Mech. Arct. Eng.*, *122*(4), 294-300. https://doi.org/10.1115/1.1320440

19- Johansson, P. I. (1976). *A finite element model for dynamic analysis of mooring cables* (Doctoral dissertation, Massachusetts Institute of Technology).

20- Palomo, M. (2017). Describing Reality: Bernoulli's Challenge of the Catenary Curve and its Mathematical Description by Leibniz and Huygens. *The Dialogue Between Sciences, Philosophy and Engineering: New Historical and Epistemological Insights. Homage to Gottfried W. Leibniz and 1646–2016*, 334.

21- Faltinsen, O. (1993). *Sea loads on ships and offshore structures* (Vol. 1). Cambridge university press.
22- Wu, Y., Wang, T., Eide, Ø., & Haverty, K. (2015). Governing factors and locations of fatigue damage on mooring lines of floating structures. *Ocean Engineering*, *96*, 109-124. https://doi.org/10.1016/j.oceaneng.2014.12.036
23- Krolikowski, L. P., & Gay, T. A. (1980, May). An improved linearization technique for frequency domain riser analysis. In *Offshore Technology Conference* (pp. OTC-3777). OTC.
24- Azizi, F., Kazemi, S. & Azarsina, F. (2024). Numerical Analysis of Catenary and Taut Mooring System Combination Effects on Heave and Pitch Motion Responses of a Semi-submersible Offshore Platform. *Journal Of Marine Engineering*, 20(43), 55-69.
http://marine-eng.ir/article-1-1120-en.html
25- Vander Velde, W. E. (1968). Multiple-input describing functions and nonlinear system design. *McGraw lill*.
26- https://en.wikipedia.org/wiki/Genetic_algorithm.
27- Aamo, O. M., & Fossen, T. I. (2000). Finite element modelling of mooring lines. *Mathematics and computers in simulation*, *53*(4-6), 415-422. https://doi.org/10.1016/S0378-4754(00)00235-4
28- DNV GL. (2017). SESAM Theory Manual—*DeepC Deep Water Coupled Floater Motion Analysis*, Version 5.2-02.
29- Ormberg, H., Fylling, I. J., Larsen, K., & Soedahl, N. (1997, April). Coupled analysis of vessel motions and mooring and riser system dynamics. In *PROCEEDINGS OF THE INTERNATIONAL CONFERENCE ON OFFSHORE MECHANICS AND ARCTIC ENGINEERING* (pp. 91-100). American Society of Mechanical Engineers.
30- Sabziyan, H., Ghassemi, H., Azarsina, F., & Kazemi, S. (2015). Appropriate model for mooring pattern of a semi-submersible platform. Journal of Subsea and Offshore-Science and Engineering, 1(1), 18-25.
31- Rashidi, J.,Ahmadi ,A.,Seif, M., & Azarsina, F. (2015, May). The effect of different bracing patterns on the behavior of semi-submersible platform. The 6th International Conference of Offshore Industries, Sharif University of Technology. (In Persian)
32- Mohseni, A. S., & Mostafa, G. B. A. (2012). The effect of heave plates on hydrodynamic behavior of Amir Kabir semi-submesible platform. The 10th international conference of coasts, ports and marine structures in Tehran. (In Persian)
33- Dardel, M., & Ghafari, H. (2018). Effects of Buoy size on the frequency and time response in catenary mooring systemof the semi -submersible platform, Modares Mechanical Engineering, Vol. 18, No. 0 2, pp. 2 0 9 -21 8, 2018 (in Persian)
34- API RP 2SK, *Recommended Practice for Design and Analysis of Stationkeeping Systems for Floating Structures, third ed*., *American Petroleum Institute,* 2005. Addendum 2008; Reaffirmed 2015.